Electronic Supplementary Information (†ESI)

Implantable Nonenzymatic Glucose/O_2 Micro Film Fuel Cell Assembled with Hierarchical AuZn Electrodes

Hui-Bog Noh,[a] M. Halappa Naveen,[a] Yong-Jin Choi,[a] Eun Sang Choe[b] & Yoon-Bo Shim*[a]

[a] Department of Chemistry and Institute of Biophysio Sensor Technology (IBST), Pusan National University, Busan 609-735, South Korea.

[b] Departments of Biological Sciences, Pusan National University, Busan 609-735, South Korea.

* Correspondence should be addressed to Yoon-Bo Shim ybshim@pusan.ac.kr

Table of contents:

1. Materials and methods

Materials: $HAuCl_4 \cdot 3 \cdot H_2O$ (≥ 99.9%), $ZnCl_2$ (99.999%), $NiSO_4$ (99%), $CoCl_2 \cdot 4H_2O$ (98%), Na_2SO_4 (99.99+%), NaOH (≥98.0%), Nafion perfluorinated ion-exchange resin (5 wt.%), and D-(+)-glucose were purchased from Sigma-Aldrich Chemical Co. (USA). Tecoflex polyurethane (TPU, SG-80A) was purchased from Thermedics (Woburn, MA). N_2 and O_2 (99.999%) gases were used as received from P. S. Chem (S. Korea). The electrochemical measurements were performed in phosphate buffer solution (PBS, pH 7.4 20 mM phosphate buffered 0.14 M NaCl). All aqueous solutions were prepared in doubly distilled water obtained from a Milli-Q water purifying system (18 MΩ cm). All other reagents were the best commercially available.

Instrumental: The electrodeposition of Au, Zn, AuZn, AuNi, and AuCo materials and the voltammetric experiments were performed on a Kosentech Model KST-P1 (S. Korea). RDE HVs were collected using a Kosentech bipotentiostat (model Bipot-1) with the EG&G PAR model 636 RDE system. Glassy carbon (GC), Pt, Au (diameter = 3.0 and 5.0 mm), Ag/AgCl (in saturated KCl), and Pt wire were used as working, reference, and counter electrodes, respectively. The FC experiments were performed in a one-electrode cell using an all-in-one carbon screen-printed micro film electrode (SPME). Modified carbon (area = 0.07 cm^2) was used as the working electrode. Carbon and silver inks were purchased from Jujo Chemical (Japan). The SPMEs were printed on polystyrene-based film using a screen printer (BANDO industrial, S. Korea). SEM images were obtained using a Cambridge Stereoscan 240 and VEGA 3 SB (Tescan Inc., USA). XRD (X'pert PRO MRD system model) was used to determine the AuZn metal phase of the deposition. EDXS analysis was performed to determine the Au to transition metal ratio. XPS experiments were performed using a VG Scientific ESCALAB 250 XPS spectrometer with a monochromatic Al Kα source, including charge compensation at the Korea Basic Science Institute (KBSI, Busan, S. Korea). TOF-SIMS experiments were performed with a TOF-SIMS 5 (ION TOF GmbH, Germany) using a bismuth liquid metal ion source. The primary analysis beam was a 25.0 keV Bi^{3+} beam that was operated in the Burst Alignment mode with a 10.0 kHz repetition rate and a pulse width of 100.0 ns. The target current was <0.2 pA when using a Faraday cup with a grounded sample holder, and the spot size was estimated to be ~300 nm. The mass range was 0 - 800 amu, with unit mass resolution, and a 256.0 x 256.0 pixel image resolution was used. The analysis area (field of view: 50.0 µm x 50.0 µm) was a randomly scanned image of the primary ions, and the primary ion dose was kept below 10^{12} ions cm^{-2} to ensure static SIMS conditions. Positive ion spectra were internally calibrated using H^+, H_2^+, CH_3^+, $C_2H_3^+$, and $C_3H_4^+$ signals. An HPLC (Aglilent 1200 series, Agilent, USA) system combined with packed columns (SUPELCOGEL C-610H, Agilent, USA) and an ESI-MS detector (HCT Basic System, Bruker, Germany) was employed to detect the products. A stereotaxic frame from the Stoelting Co. (model 620, USA) was used for holding the animal (rat) in place while running the experiment.

Preparation of dendrite catalysts: Au, Zn, AuZn, AuNi, and AuCo bimetal dendrites were electrochemically prepared, and the catalytic characteristics were compared towards both the ORR and the glucose oxidation reactions, where the bimetal components were chosen due to the similar preparation conditions and catalytic properties for the FC reactions. Prior to electrodeposition, the GC electrode was polished to a mirror finish with 0.5 μm alumina powder and a polishing cloth, and then it was rinsed with distilled water. Au and Zn dendrites were prepared in a 0.1 M Na_2SO_4 solution containing 10.0 mM $HAuCl_4 \cdot 3H_2O$ and 30.0 mM $ZnCl_2$ at the deposition potential of -500.0 mV for 1000.0 s. AuZn, AuNi, and AuCo bimetal dendrites were prepared from 10.0 mM $HAuCl_4 \cdot 3H_2O$ and 30.0 mM $ZnCl_2$, $NiSO_4$, and $CoCl_2 \cdot 4H_2O$, respectively, and the pH was maintained at 4.0 using NaOH. The deposition potentials for AuZn, AuNi, and AuCo bimetal dendrites were -500.0, -600.0, and -700.0 mV, respectively for 1000.0 s. The mixed solution was purged with N_2 gas for 30 min before the electrodeposition process. Then, the electrodes were washed successively with 0.1 M HCl, acetone, ethanol, and water several times. The experimental parameters were optimized in terms of the concentration of analytes, deposition time, deposition potential, and pH, which all affect the dendrite formation and catalytic activity.

Implantable micro FC test in rats: Adult male Sprague-Dawley rats (200 - 250 g) were obtained from Hyo-Chang Science Co. (Korea). The procedures on the animals were approved by the Institutional Animal Care and Use Committee, and were in accordance with the provisions of the NIH "Guide for the Care and Use of Laboratory Animals". The rats were humanely killed after each *in vivo* measurement. Test procedures were carried out in accordance with a previous work.[S1]

Method for implantation of the micro FC in rats: Male Wistar rats weighing 300 - 560 g were anesthetized with combination of Zoletil 50 (Virbac, S. Korea) and Rompun (Bayer Korea, S. Korea) (1:4 v/v). Dissection for the implantation of FC was performed in the abdominal cavity, subcutaneous layer of neck and brain of rats. The FC was subcutaneously pushed into the abdominal cavity, subcutaneous layer and brain (see manuscript Fig. 3). The wires were then soldered to a microconnector. Long-term stability of the FC implanted in the brain of rat was tested. Carboxylate cement was used as the covering material for restraining the implanted FC in place. While abdominal cavity or subcutaneous layer was finally sutured. The animals were immediately sacrificed after measurements.

FC assembly and power measurements: The AuZn bimetal was used for both anode and cathode of the GOFC in the alkaline (0.1 M NaOH). In case of *in vivo* and *in vitro* experiments in the physiological solution (pH 7.4, containing Cl^-), the polymer (0.5% Nafion and 3% polyurethane) coated AuZn electrode was used as anode and cathode. The FC system, assembled in our laboratory, was operated at open-circuit voltage. A Nafion membrane (115, NanoBest Corp. Korea) was placed between the anode and cathode. Glucose and whole blood, used as anodic fuels, were injected at a rate

of 0.6 mL/min into the corresponding compartment of the cell using a Masterflex model (Cole-Parmer Instrument Co. USA). O_2 gas was used as the cathodic fuel in all the *in vitro* measurements.

In case of *in vivo* experiments, a set of two micro film electrodes facing each other (gap between electrodes was around 100 µm) were used for the subcutaneous layer of neck and brain of rat, where the anode and cathode were separated with chemical tissue. Otherwise, polymer/AuZn assembled on the GCE was used for implanting in the abdominal cavity. All electrodes were activated in a 10.0 mM glucose solution before experiments. For abdominal cavity experiment, a pair of electrodes were wrapped in perforated silicone tube. Miniaturized insulated brass wires (UBA3219, Industrifil) were connected to each GC (cell size: 8 mm x 4 mm, diameter: 5.0 mm) and SPME (cell size: 4 mm x 6 mm, thickness: 1 mm, diameter: 3.0 mm) with an external connection (see †ESI Fig. S8 and manuscript Fig. 3(A)).

The voltage and current generated by the FC were measured with the help of an external variable resistance load (model RM6-N, CROPICO, UK), a digital multimeter (model DM-334, EZ Digital, USA), and a battery cycler (model WBCS3000, WonATech Co. Ltd., S. Korea). The performance of the cell was evaluated from current curves obtained at open-circuit voltage.

2. LSVs recorded for the catalytic electrodes in N_2 and O_2 saturated

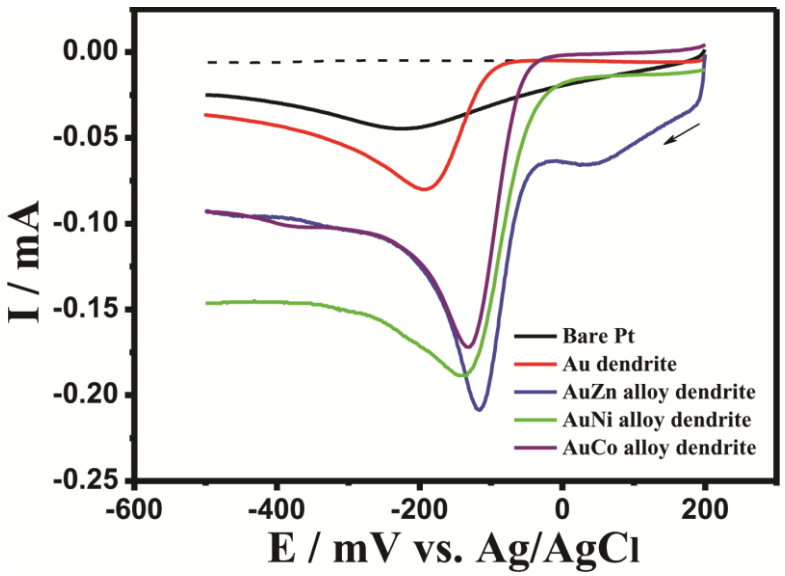

Fig. S1. LSVs recorded for bare Pt, Au dendrite, AuZn, AuNi, and AuCo bimetal dendrites electrodes in a 0.1 M NaOH solutions with N_2 (dash line) and O_2 saturated (solid line) at 50.0 mVs^{-1}.

3. The number of electrons transfer (*n*) was calucalated using the Koutecky-Levich equation

$$\frac{1}{J} = \frac{1}{J_{kin}} + \frac{1}{J_{diff}} = \frac{1}{J_{kin}} + \frac{1}{B\sqrt{\omega}} \quad (1)$$

$$B = 0.62nFD^{2/3}\nu^{-1/6}C \quad (2)$$

where n is the number of electrons transferred during the ORR, F is the Faraday constant, D is the diffusion coefficient of O_2 in the 0.1 M NaOH electrolyte (D = 1.9 × 10^{-5} cm^2s^{-1}), C is the bulk concentration of O_2 (C = 1.2 × 10^{-3} $mMcm^{-3}$), and ν is the kinetic viscosity of the electrolyte (ν = 1.0 × 10^{-2} cm^2s^{-1}).

4. HVs recorded for the polymer/AuZn in the O_2 saturated physiological medium

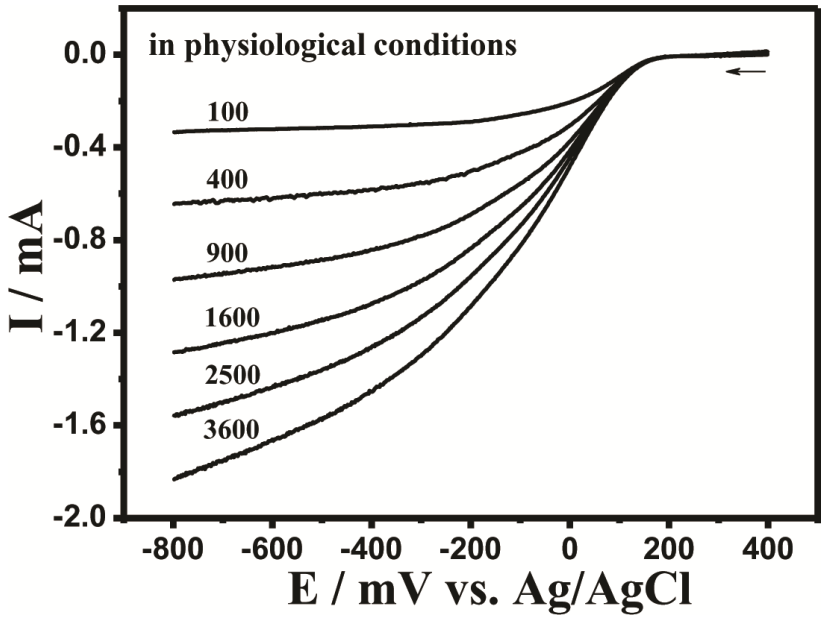

Fig. S2. HVs recorded for the ORR of polymer/AuZn dendrite according to the rotation rates (rpm: 100, 400, 900, 1600, 2500, and 3600).

5. Voltammetric behaviors of the glucose oxidation on the electrodes

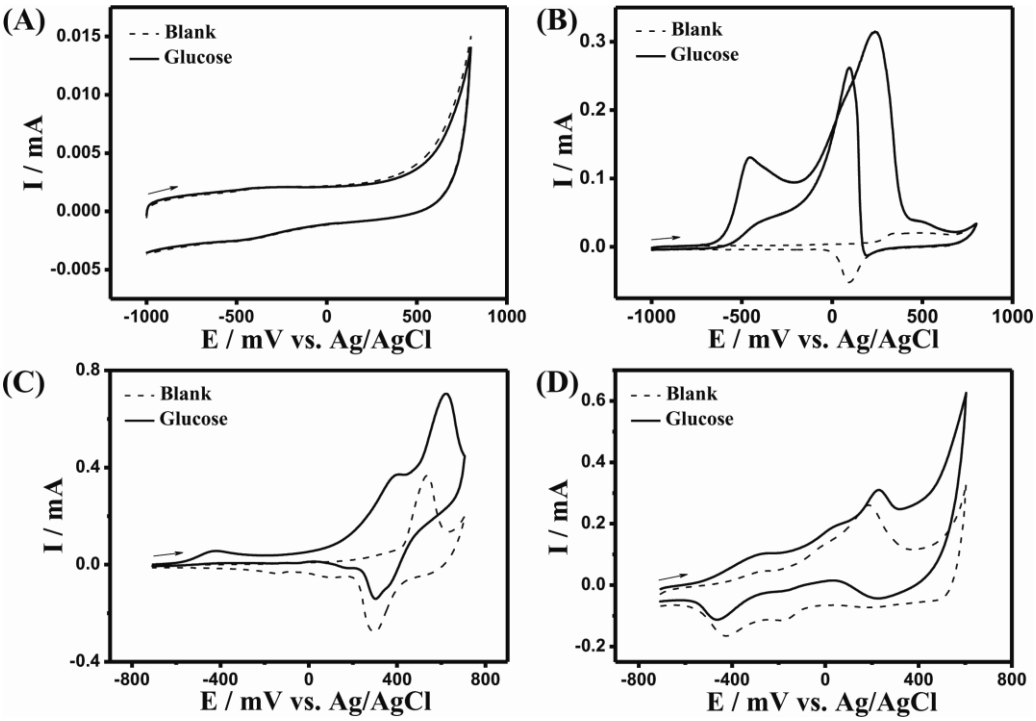

Fig. S3. CVs recorded for (A) bare GC, (B) bare Au, (C) AuNi, and (D) AuCo dendrites electrodes in a 0.1 M NaOH solution (dash line) containing 10.0 mM glucose (solid line) at scan rate of 50.0 mVs^{-1}.

6. Electrocatalytic oxidation of glucose on the dendrite electrodes

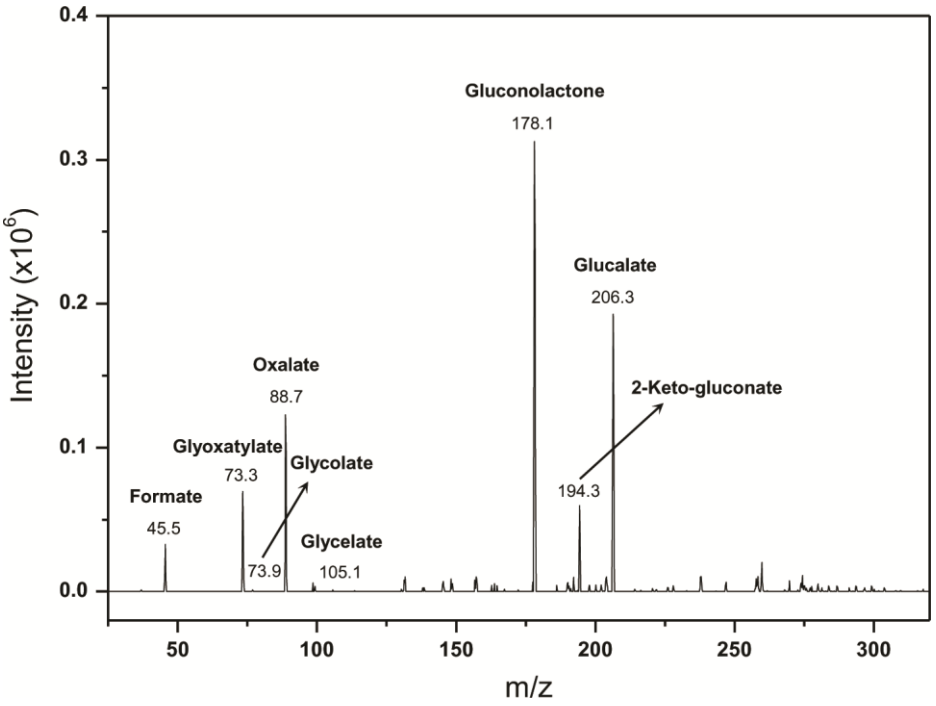

Fig. S4. PLC-ESI MS spectrum for products of oxidized glucose.

7. XPS analysis

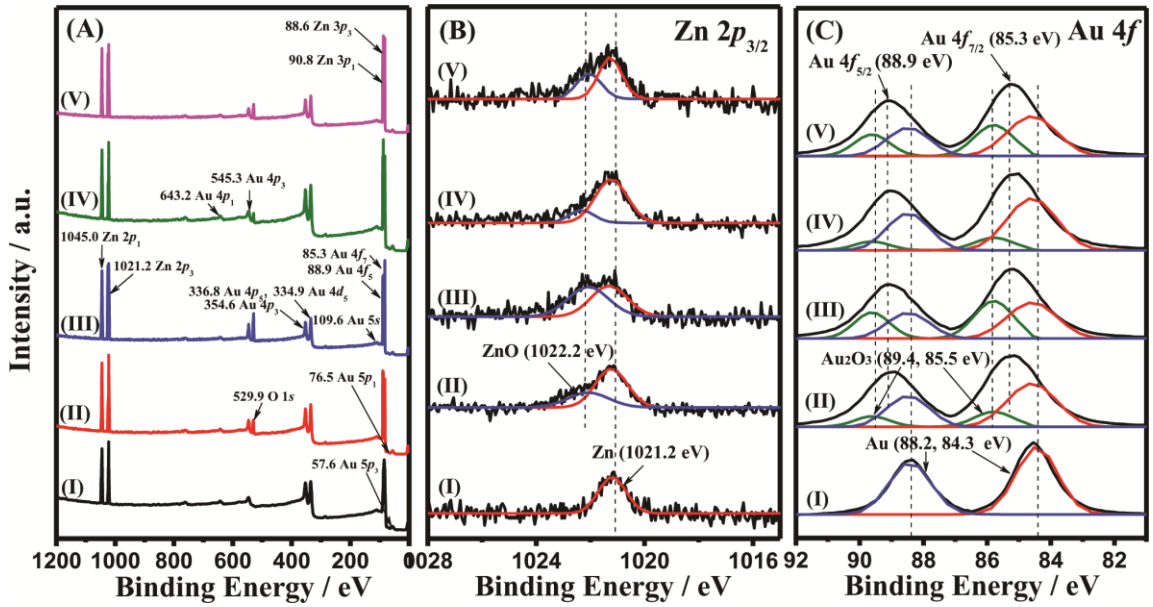

Fig. S5. XPS (A) survey spectrum, (B) Zn $2p_{3/2}$, and (C) Au $4f_{(5/2, 7/2)}$ peaks for AuZn dendrite: (I) bare dendrite, after oxidation in (II) 0.1 M NaOH and (III) glucose solution, and after reduction in (IV) 0.1 M NaOH and (V) O_2 saturated solution.

8. Schematic diagram and performance of GOFC

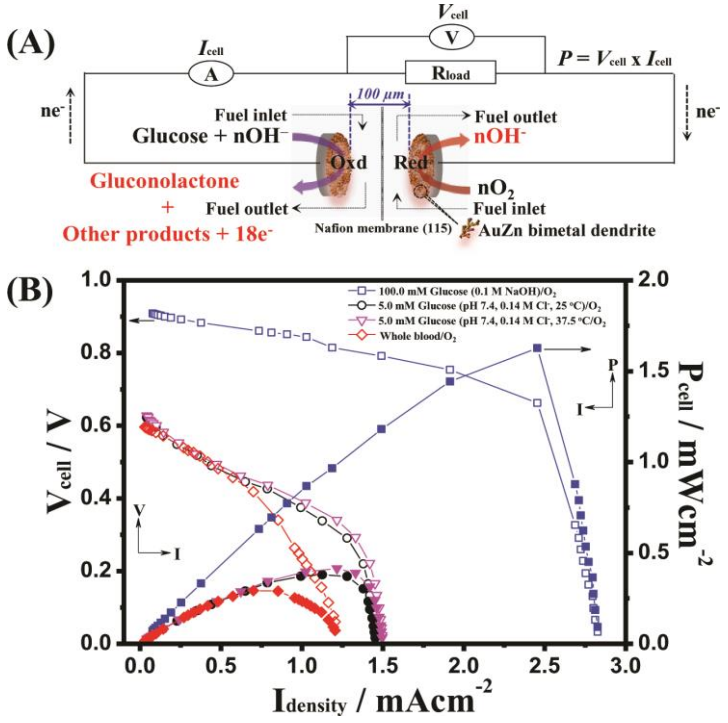

Fig. S6. (A) Schematic diagram of a GOFC system. (B) *I-V* and *I-P* curves for glucose in 0.1 M NaOH (25 ^{o}C), whole blood (25 ^{o}C), and physiological conditions (pH 7.4, 25 and 37.5 ^{o}C).

9. Optimization of the experimental parameters for analysis

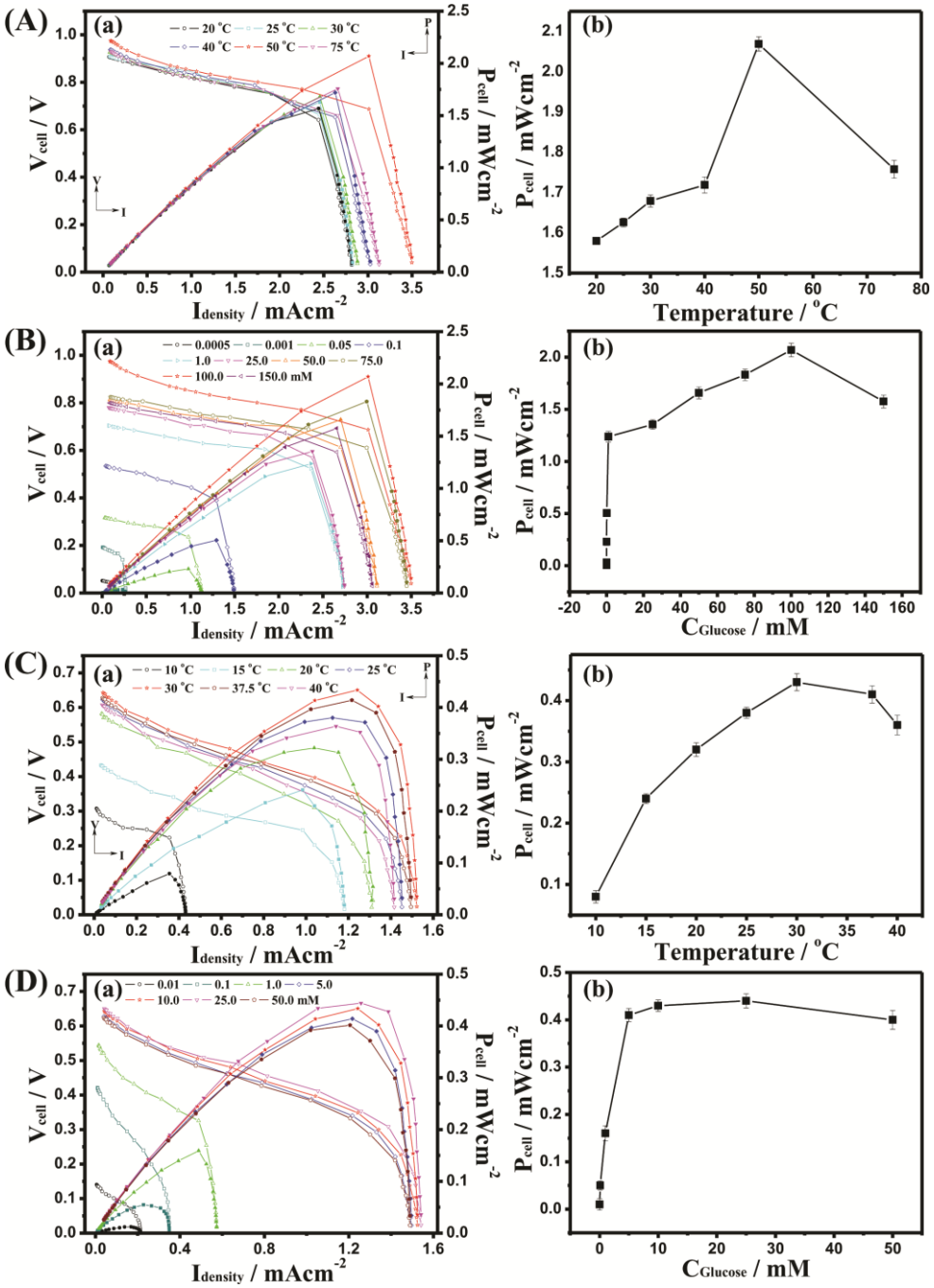

Fig. S7. (A(a)) *I-V* and *I-P* curves for 100.0 mM glucose and (A(b)) the plot for the power density in 0.1 M NaOH, according to the temperatures from 20 to 75 °C. (B(a)) *I-V* and *I-P* curves and (B(b)) the plot for the power density in 0.1 M NaOH, according to the glucose concentrations (500.0 nM - 150.0 mM) at 50 °C. (C(a)) *I-V* and *I-P* curves for 5.0 mM glucose and (C(b)) the plot for the power density under physiological conditions, according to the temperatures from 10 to 40 °C. (D(a)) *I-V* and *I-P* curves and (D(b)) the plot for the power density under physiological conditions, according to the glucose concentrations (0.01 - 50.0 mM) at 37.5 °C.

Table S1. Performances of the GOFCs under different conditions *(n = 3).*

Electrolytes	Parameters		Composition of the FCs		Cell voltage, *V* (V) (± SD)	RSD, %	Current density, *I* ($mAcm^{-2}$) (± SD)	RSD, %	Power density, *W* ($mWcm^{-2}$) (± SD)	RSD, %
			Anodes	Cathodes						
0.1 M NaOH	Temperatures, ^{o}C	20	AuZn bimetal/GCE		0.91 (± 0.04)	4.40	2.82 (± 0.10)	3.55	1.57 (± 0.08)	5.10
		25			0.91 (± 0.05)	5.49	2.83 (± 0.11)	3.89	1.63 (± 0.08)	4.91
		30			0.93 (± 0.05)	5.38	2.88 (± 0.14)	4.86	1.68 (± 0.08)	4.76
		40			0.94 (± 0.03)	3.19	3.03 (± 0.15)	4.95	1.72 (± 0.06)	3.49
		50			0.98 (± 0.04)	4.08	3.50 (± 0.17)	4.86	2.07 (± 0.08)	3.86
		75			0.93 (± 0.03)	3.23	3.13 (± 0.15)	4.79	1.76 (± 0.08)	4.55
	Concentrations of glucose, mM (50 ^{o}C)	150.0			0.80 (± 0.03)	3.75	3.06 (± 0.11)	3.59	1.58 (± 0.06)	3.80
		100.0			0.98 (± 0.04)	4.08	3.50 (± 0.17)	4.86	2.07 (± 0.08)	3.86
		75.0			0.83 (± 0.04)	4.82	3.45 (± 0.20)	5.80	1.83 (± 0.09)	4.92
		50.0			0.81 (± 0.05)	6.17	3.11 (± 0.13)	4.18	1.66 (± 0.07)	4.22
		25.0			0.78 (± 0.05)	6.41	2.74 (± 0.17)	6.20	1.36 (± 0.05)	3.68
		1.0			0.70 (± 0.04)	5.71	2.72 (± 0.08)	2.94	1.24 (± 0.04)	3.23
		0.1			0.54 (± 0.03)	5.56	1.49 (± 0.08)	5.37	0.51 (± 0.02)	3.92
		0.05			0.32 (± 0.02)	6.25	1.13 (± 0.05)	4.42	0.23 (± 0.01)	4.35
		0.001			0.19 (± 0.01)	5.26	0.27 (± 0.02)	7.41	0.03 (± 0.002)	6.67
		0.0005			0.05 (± 0.003)	6.00	0.15 (± 0.010)	6.67	0.01 (± 0.001)	6.82
Physiological conditions (pH 7.4, containing 0.14 M Cl^{-})	Temperatures (^{o}C)	10	Polymer/AuZn bimetal/GCE		0.31 (± 0.02)	6.45	0.43 (± 0.02)	4.66	0.08 (± 0.004)	5.02
		15			0.43 (± 0.02)	4.65	1.18 (± 0.05)	4.24	0.24 (± 0.01)	4.17
		20			0.58 (± 0.03)	5.17	1.31 (± 0.06)	4.58	0.32 (± 0.01)	3.13
		25			0.62 (± 0.03)	4.83	1.45 (± 0.06)	4.14	0.38 (± 0.02)	5.26
		30			0.64 (± 0.04)	6.25	1.52 (± 0.08)	5.26	0.43 (± 0.03)	6.98
		37.5			0.63 (± 0.04)	5.98	1.50 (± 0.07)	4.65	0.41 (± 0.03)	6.25
		40			0.61 (± 0.04)	7.27	1.42 (± 0.05)	3.20	0.36 (± 0.02)	6.45
	Concentrations of glucose, mM (37.5 ^{o}C)	50.0			0.62 (± 0.02)	3.23	1.49 (± 0.08)	5.37	0.40 (± 0.02)	5.07
		25.0			0.65 (± 0.03)	4.62	1.54 (± 0.04)	2.60	0.44 (± 0.02)	4.55
		10.0			0.64 (± 0.03)	5.12	1.53 (± 0.09)	5.65	0.43 (± 0.03)	6.12
		5.0			0.63 (± 0.04)	5.98	1.50 (± 0.07)	4.65	0.41 (± 0.03)	6.25
		1.0			0.54 (± 0.02)	3.70	0.57 (± 0.03)	5.26	0.16 (± 0.01)	6.25
		0.1			0.42 (± 0.02)	4.76	0.35 (± 0.01)	2.86	0.05 (± 0.003)	6.12
		0.01			0.21 (± 0.01)	4.76	0.14 (± 0.01)	7.14	0.01 (± 0.001)	6.52

Electrode area: 0.196 cm^{2}; Flow rate of fuel: 0.6 mL/min; Glassy carbon electrode (GCE); Standard deviation (SD); Relative standard deviation (RSD).

10. Assembly of FC implanted in the abdominal cavity

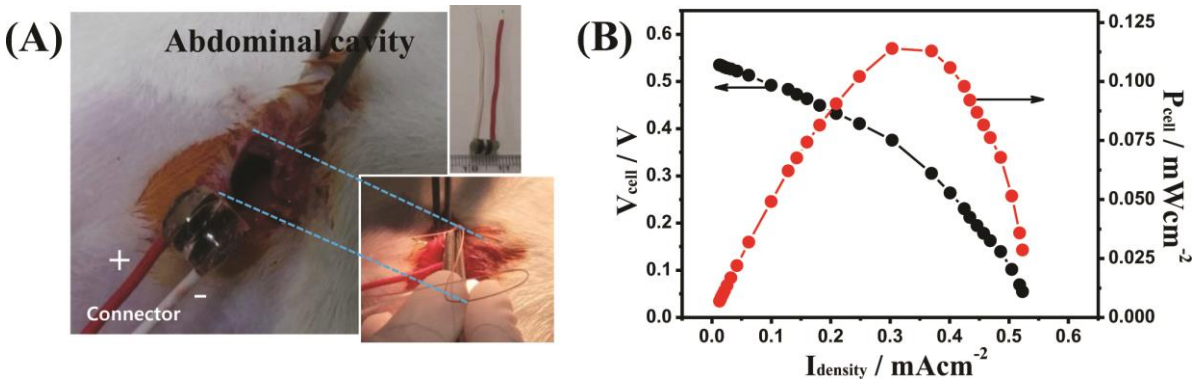

Fig. S8. (A) Polymer/AuZn with GC electrode wrapped in perforated silicone tube electrodes. Electrical connection of the FC in Wistar rats; the output wires are fixed to the stand. (B) *I-V* and *I-P* curves from FC.

11. Comparison of the electrical outputs for implanted fuel cells

Table S2. Comparison of the electrical outputs for implanted fuel cells operating *in vivo*[a].

Animal/location	Composition of the FCs		V_{oc}/mV	I_{sc}/μA	P_{max}/μW	Ref.
	Anodic catalysts	Cathodic catalysts				
Human/whole blood (*In vitro*)	AuZn bimetal	AuZn bimetal	596.2	236.2	57.4	This work
Rat/abdominal cavity			534.9	102.5	22.3	This work
Rat/subcutaneous layer of neck			518.7	23.1	6.8	This work
Rat/brain			550.0	33.1	7.7	This work
Pig/venous blood	Pt	Graphene/stainless steel mesh	314.16	-	2.5	S2
Clam/hemolymph	Glucose dehydrogenase	Laccase	350.0	80.0	10.0	S3
Insect (blaberus discoidalis)/abdomen	Glucose oxidase	Bilirubin oxidase	-	-	0.07	S4
Lobster/hemolymph	Glucose dehydrogenase	Laccase	540.0	1000.0	160.0	S5
Rat/abdominal cavity	Glucose oxidase	Laccase	570.0	-	38.7	S6
Rat/cremaster tissue	Glucose dehydrogenase	Laccase	140.0	10.0	0.35	S7
Rabbit/ear vein	Glucose dehydrogenase	Bilirubin oxidase	810.0	1.5	0.42	S8
Rat/retroperitoneal space	Glucose oxidase	Polyphenol oxidase	270.0	-	2.0	S9
Snail/hemolymph	Glucose dehydrogenase	Laccase	530.0	42.5	7.45	S10

[a] The numbers given in the table were derived from the original published values taking into account the electrode geometrical areas. For some implanted fuel cells the electrode areas were not reported, thus current and power cannot be derived from the published values of the current density and power density.

12. References

S1. Md. A. Rahman, N. -H. Kwon, M. -S. Won, E. S. Choe and Y. -B. Shim, *Anal. Chem.*, 2005, **77**, 4854.

S2. T. Sharma, Y. Hu, M. Stoller, M. Feldman, R. S. Ruoffx, M. Ferrari and X. Zhang, *Lab Chip*, 2011, **11**, 2460.

S3. A. Szczupak, J. Halamek, L. Halamkova, V. Bocharova, L. Alfonta and E. Katz, *Energy Environ. Sci.*, 2012, **5**, 8891.

S4. M. Rasmussen, R. E. Ritzmann, I. Lee, A. J. Pollack and D. Scherson, *J. Am. Chem. Soc.*, 2012, **134**, 1458.

S5. K. MacVittie, J. Halamek, L. Halamkova, M. Southcott, W. D. Jemison, R. Lobel and E. Katz, *Energy Environ. Sci.*, 2013, **6**, 81.

S6. A. Zebda, S. Cosnier, J. -P. Alcaraz, M. Holzinger, A. Le Goff, C. Gondran, F. Boucher, F. Giroud, K. Gorgy, H. Lamraoui and P. Cinquin, *Sci. Rep.*, 2013, **3**, 1516.

S7. J. A. Castorena-Gonzalez, C. Foote, K. MacVittie, J. Halamek, L. Halamkova, L. A. Martinez-Lemus and E. Katz, *Electroanalysis*, 2013, **25**, 1579.

S8. T. Miyake, K. Haneda, N. Nagai, Y. Yatagawa, H. Onami, S. Yoshino, T. Abe and M. Nishizawa, *Energy Environ. Sc*i., 2011, **4**, 5008.

S9. P. Cinquin, C. Gondran, F. Giroud, S. Mazabrard, A. Pellissier, F. Boucher, J. -P. Alcaraz, K. Gorgy, F. Lenouvel, S. Mathe, P. Porcu and S. Cosnier, *PLoS One*, 2010, **5**, e10476.

S10. L. Halamkova, J. Halamek, V. Bocharova, A. Szczupak, L. Alfonta and E. Katz, *J. Am. Chem. Soc.*, 2012, **134**, 5040.